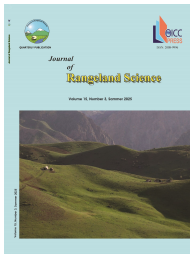

Volume 15, Issue 3, 152527 (1-14)

Journal of Rangeland Science (JRS)

https://doi.org/10.57647/j.jrs.2025.1503.27

The influence of meteorological fluctuations on vegetation dynamics: Trends and modeling

Pouyan Dehghan Rahimabadi, Setareh Bagheri, Sahar Nasabpour Molaei, Hemed Joneidi Jafari, Hassan Khosravi*, Hossein Azarnivand

Department of Arid and Mountainous Regions Reclamation, University of Tehran, Tehran, Iran.

***Corresponding author:** hakhosravi@ut.ac.ir

Original Research

Received:
22 May 2023
Revised:
30 July 2024
Accepted:
17 October 2024
Published online:
20 July 2025

Abstract:

Climate fluctuations can influence the density, health, and vulnerability of vegetation, highlighting the need to evaluate their combined impacts on vegetation dynamics. This study analyzed the trends of changes in precipitation and temperature in West and East Azerbaijan provinces, Iran, to clarify complex interactions of both climatic variables and indices with vegetation cover. The trend of precipitation, temperature, Standardized Precipitation Index (SPI), and Rainfall Anomaly Index (RAI) were analyzed and their impacts on vegetation dynamics were modeled from 1987 to 2022. The maps of Enhanced Vegetation Index (EVI) derived from Landsat 5 (TM + MSS), Landsat 7 (TM + ETM) and Landsat 8 OLI were adopted to examine the effect of climate fluctuations on vegetation cover. The results indicated a decreasing trend in precipitation and an increasing trend in temperature. A negative correlation was found between precipitation and temperature ($r = -0.88$) ($p < 0.01$). Additionally, there were positive correlations between EVI and precipitation ($r = 0.53$), EVI and SPI ($r = 0.57$) and between EVI and RAI ($r = 0.61$) while there was no significant correlation between EVI and temperature. Moreover, the findings showed that the SPI was a reliable index in estimating vegetation conditions. The findings of this study can enhance the understanding of ecosystem responses to climate fluctuations in the study area.

Keywords: Climate fluctuations; Drought indices; Regression model; Vegetation cover

Introduction

Vegetation growth is mainly influenced by external climatic factors such as precipitation and temperature. As a result, fluctuations in climate can impact different types of vegetation in various ways. Meteorological elements profoundly affect the availability of water essential for vegetation health and growth. Below-average precipitation can have adverse effects on agriculture and forestry (Ahmadi et al., 2019), and damage natural ecosystems (Dehghan Rahimabadi et al., 2018; Buras et al., 2020). In the long term, it may even lead to soil degradation and desertification (Dehghan Rahimabadi et al., 2021). Meanwhile, temperature fluctuations could influence potential evaporation and transpiration patterns, thereby affecting the hydrological cycle (Hui-Mean et al., 2018). As a result, fluctuations in these climatic factors could alter vegetation patterns and pose risks to natural resources. Hence, studying long-term changes and trends in precipitation and temperature on global, continental, and especially regional scales is imperative for effective water resource management (Darvand et al., 2021).

Therefore, climatic-induced water shortages arising from meteorological droughts threaten vegetation's vulnerability. Drought is a phenomenon resulting from reduced precipitation and evaluated temperatures, potentially causing significant impacts on society, the environment, and the economy (Khan et al., 2021; Eskandari Damaneh et al., 2021; Eskandari Damaneh et al., 2022). However, drought is defined as a period of abnormally dry weather leading to changes in vegetation cover (Yeh, 2019). It is a transient feature of a climate anomaly resulting in below-average precipitation or limited distribution in a region (Hasan et al., 2021). Precipitation determines the onset, duration, intensity and end of drought (Vicente-Serrano et al., 2010). On the other hand, an increase in temperature leads to increased water loss and greater stress on vegetation. Therefore, it is expected that a decrease in vegetation will occur with a decrease in precipitation and an increase in temperature. Therefore, meteorological droughts severely affect vegetation by reducing soil moisture, leading to weakened vegetation health, de-

layed growth, and prolonged periods of stress. Therefore, attention to vegetation cover sensitivity in response to climate change has been introduced as a research priority in the field of rapidly accelerating global warming (Wu et al., 2023).

Meteorological indices, such as Standardized Precipitation Index (SPI) (Heydari Alamdarloo et al., 2020; Bagheri et al., 2022), Rainfall Anomaly Index (RAI) (Amiri and Gocic, 2023), Standardized Precipitation Evapotranspiration Index (SPEI) (Medeiros and Silva, 2024), and Palmer Drought Severity Index (PDSI) (Zhou et al., 2022), which utilize precipitation as a key variable, have been employed in drought analyses. On the other hand, vegetation indices like Enhanced Vegetation Index (EVI) (Dehghan Rahimabadi and Azarnivand, 2023), Normalized Difference Vegetation Index (NDVI) (Zhang et al., 2024), and Vegetation Health Index (VHI) (Kartal et al., 2024) play a significant role as they can provide information on the lack of precipitation and the resulting vegetation damage (Dehghan Rahimabadi et al., 2024).

Most previous studies on long-term climatic trends and their impact on vegetation cover have focused on temperature and precipitation. Zhang et al. (2020) observed that vegetation dynamics in the Yangtze River basin, in China are significantly controlled by the temperature of previous months. They noted a delayed effect of temperature in Spring on vegetation and emphasized the substantial impact of summer precipitation. Heydari Alamdarloo et al. (2021) stated that vegetation cover in the west and northwest of Iran shows the highest correlation with annual precipitation between 213 – 300 mm and annual mean temperatures ranging from 8 to 12 °C. Zhan et al. (2021) discovered that the vegetation responses to climatic factors in the Hanjiang River Basin, China vary notably with altitude. They observed that as altitude increases, the effect of temperature delays on vegetation diminishes gradually while the influence of precipitation delays becomes more pronounced. Dehghan Rahimabadi and Azarnivand (2023) reported that sparse vegetation cover in the Namak Lake basin, Iran, was more susceptible to meteorological fluctuations than dense vegetation cover. Dastigerdi et al. (2024) stated that in the highlands of northeastern Iran, decreasing temperatures predominantly affect vegetation, whereas, in the lowlands, reduced precipitation significantly limits vegetation growth. This study contributes to the understanding of how climatic variables and indices influence vegetation cover in the West and East Azerbaijan provinces. The primary objective was to analyze fluctuations in precipitation, temperature, SPI, and RAI and to model their impacts on vegetation dynamics. The results of this study can assist in developing effective strategies to preserve and protect vegetation and promote its growth under variations in climatic variables.

Materials and methods

Study area

The study area encompasses the West and East Azerbaijan provinces, Iran, situated between 35° 58′ and 39° 46′N latitude and 44° 02′ and 48° 21′E longitude. It spans an area of 87594.6 km^2, representing about 5.3% of Iran's total area, with Urmia Lake covering 4594.8 km^2 of the region. This region is one of Iran's mountainous areas with diverse and extensive topography (figure 1). Due to its natural structure, various special ecosystems with a range of plant

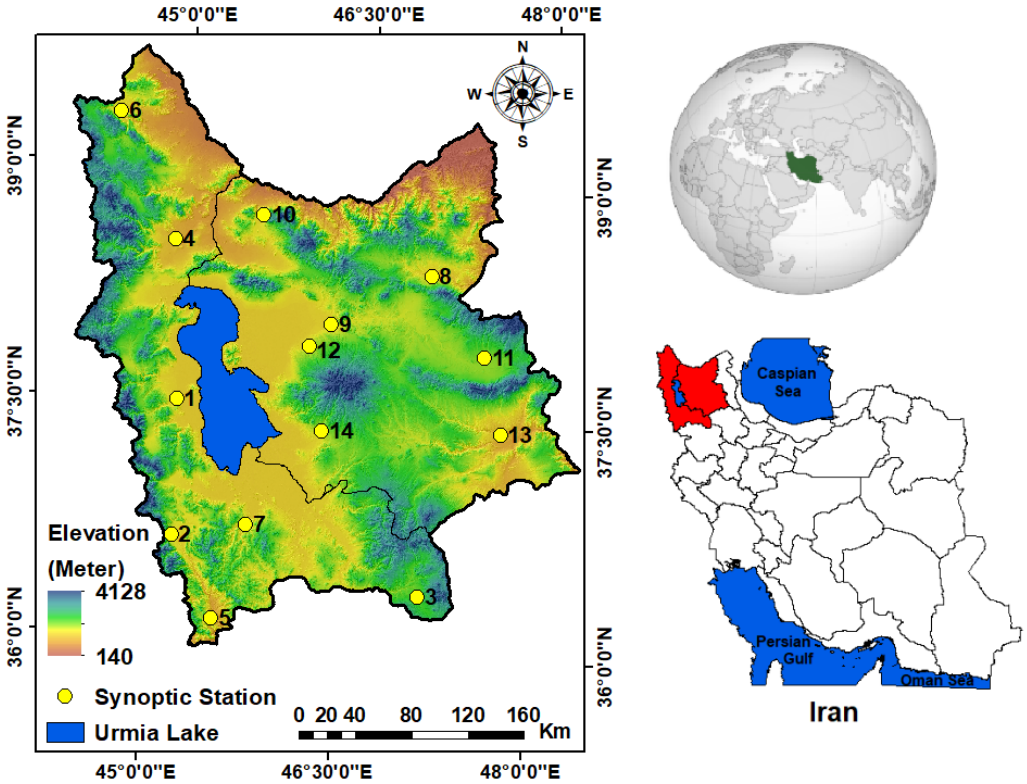

Figure 1. Geographical location of the West and East Azerbaijan provinces in Iran.

combinations have developed at different topographic levels, particularly in the form of rangelands (Saberi and Soltani-Gerdefaramarzi, 2017). The climate is moderate, with an average annual precipitation of approximately 350 mm and a mean monthly temperature of 12.5 °C (www.irimo.ir). The agricultural area is estimated to be about 21000 km^2, which constitutes approximately 6.12% of Iran's cultivated land area (Farajnia and Moravej, 2020).

Additionally, the Land Use Land Cover (LULC) map of the study area derived from the LULC map prepared by the Natural Resources and Watershed Management Organization of Iran includes agricultural land, dense forest, moderate forest, sparse forest, good rangeland, moderate rangeland, poor rangeland, urban area, rock, salt land, and water body (figure 2). Table 1 demonstrates the area of each type.

Table 1. The area of LULC classes.

LULC	Area	
	km^2	Percent (%)
Agricultural land	35140.5	40.12
Dense forest	818.5	0.93
Moderate forest	1695.4	1.94
Spare forest	1012.2	1.16
Good rangeland	10359.8	11.83
Moderate rangeland	13488.1	15.4
Poor rangeland	17890.1	20.42
Urban area	536.0	0.61
Rock	54.8	0.06
Salt land	1440.0	1.64
Waterbody	5159.2	5.89
Total area	87594.6	100

Data collection

In this study, meteorological data including monthly precipitation and temperature from fourteen synoptic stations existing in the study area from 1987 to 2022 were utilized to analyze the trend of these two important climatic variables and their effects on vegetation cover (Table 2).

Additionally, monthly Enhanced Vegetation Index (EVI) data were from the spectral bands of Landsat 5 (TM + MSS), Landsat 7 (TM + ETM), and Landsat 8 OLI for the spring of 1987 to 2017 at five-year intervals. In the study area, vegetation cover reaches its peak during spring; therefore, the mean EVI maps for April, May, and June were utilized. Table 3 presents the specifications of the satellite images.

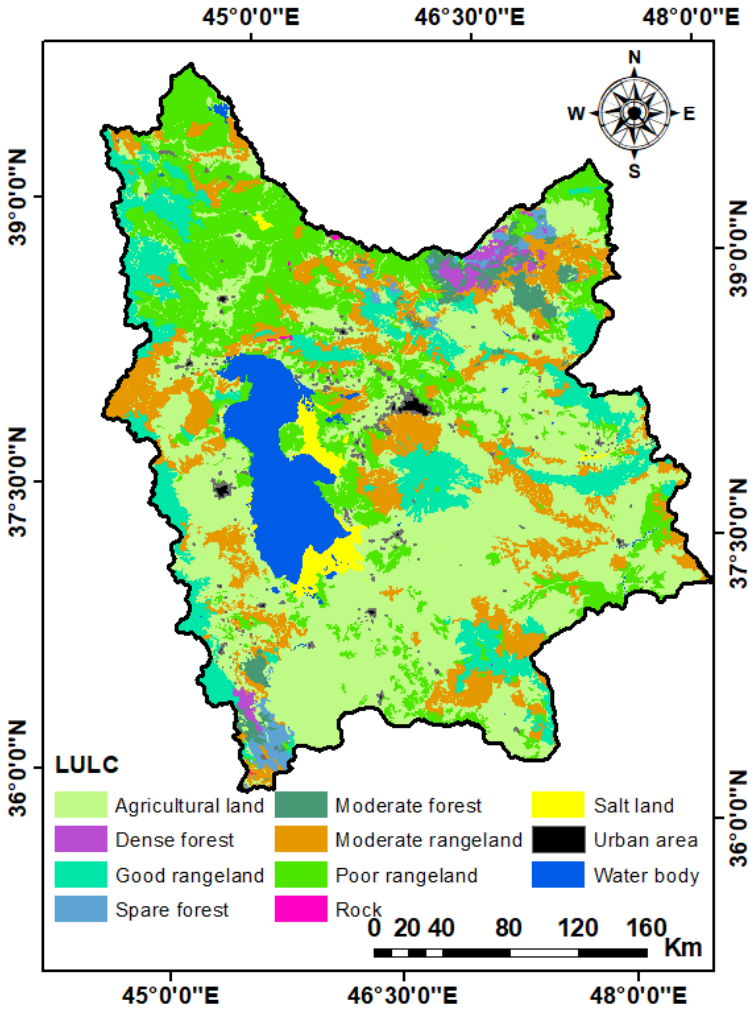

Figure 2. LULC map of the West and East Azerbaijan provinces.

Table 2. The characteristics of the synoptic stations.

Row	Meteorological station	Longitude (E)	Latitude (N)	Altitude (m)	Mean annual precipitation (mm)	Mean monthly temperature (°C)
1	Urmia	45° 05′	37° 32’	1315.9	310.1	11.6
2	Piranshahr	45° 08′	36° 40′	1455.0	688.0	13.5
3	Takab	47° 07′	36° 23′	1765.0	324.8	10.3
4	Khoy	44° 58′	38° 33′	1103.0	262.3	12.9
5	Sardasht	45° 30′	36° 09′	1670.0	830.7	13.7
6	Maku	44° 26′	39° 20′	1411.3	299.1	10.9
7	Mahabad	45° 43′	36° 46′	1385.0	396.8	13.4
8	Ahar	47° 04′	38° 26′	1390.5	283.4	11.1
9	Tabriz	46° 17′	38° 05′	1361.0	260.0	12.9
10	Jolfa	45° 40′	38° 45′	736.2	205.3	15.2
11	Sarab	47° 32′	37° 56′	1682.0	238.5	09.4
12	Sahand	46° 07′	37° 26′	1641.0	206.3	12.3
13	Mianeh	45° 08′	36° 40′	1110.0	272.4	14.4
14	Maragheh	47° 42′	37° 27′	1477.7	279.6	13.3

Methodology

In this study, climatic variables such as precipitation and temperature, along with indices namely SPI and RAI were employed to analyze the fluctuations. Additionally, EVI was utilized to investigate changes in vegetation cover and the impact of climate fluctuations on it. Precipitation and temperature are known to significantly influence changes in vegetation.

The SPI is widely recommended for detecting, monitoring, and assessing dry and wet conditions, identifying their variability across different spatial and temporal scales (Tirivarombo et al., 2018). In the present study, monthly precipitation data for April, May, and June from 1987 to 2022 were used to calculate SPI, according to equation (2):

$$\mathrm{SPI} = \frac{P_i - \bar{P}}{\mathrm{SD}} \tag{1}$$

where:

SPI stands for Standardized Precipitation Index,

P_i represents the amount of precipitation in ith year,

SD is the standard deviation of precipitation during the studied period, and

$\bar{P}$ is the average precipitation in spring during 1987 – 2022.

The classification of SPI is presented in Table 4.

RAI was also utilized to assess precipitation conditions. Compared to SPI, RAI provides greater transparency and less complexity in evaluating drought indicators (Aryal et al., 2022). The analysis included calculating RAI to determine the duration of dry and wet periods, using equations (2) and (3).

$$\mathrm{RAI} = 3 \times \left[\frac{N - \bar{N}}{\bar{M} - \bar{N}}\right] \quad \text{for positive anomalies} \tag{2}$$

$$\mathrm{RAI} = -3 \times \left[\frac{N - \bar{N}}{\bar{X} - \bar{N}}\right] \quad \text{for negative anomalies} \tag{3}$$

where:

N represents the current monthly/yearly precipitation,

$\bar{N}$ is monthly/yearly average precipitation of the historical series (mm);

$\bar{M}$ and $\bar{X}$ signify the average of the ten highest and lowest monthly/yearly precipitations of the historical series (mm), respectively.

Positive anomalies are characterized by values above the average, while negative anomalies are defined by values below the average (Table 5).

Moreover, the EVI serves as a crucial quantitative indicator

Table 3. The means of DM yield and morphological traits in five *Astragalus* species.

Satellite	Year	Month	Path	Row	Pixel size (m × m)
Landsat 5 (TM + MSS)	1987, 1992, 1997	April, May, Jun	166, 167, 168, 169, 170	32, 33, 34, 35	30×30
Landsat 7 (TM + ETM)	2002, 2007, 2012	April, May, Jun	166, 167, 168, 169, 170	32, 33, 34, 35	30×30
Landsat 8 OLI	2017, 2022	April, May, Jun	166, 167, 168, 169, 170	32, 33, 34, 35	30×30

Table 4. Classification of SPI (Standardized Precipitation Index).

Class	Extremely dry	Severely dry	Moderately dry	Normal	Moderately wet	Very wet	Extremely wet
SPI	SPI≤-2	-2<SPI≤-1.5	-1.5<SPI≤-1	-1<SPI<1	1≤SPI<1.5	1.5≤SPI<2	SPI≤2

Table 5. Classification of RAI.

Class	Extremely dry	Very dry	Dry	Normal	Humid	Very humid	Extremely humid
RAI	RAI ≤ -4	-4 < RAI ≤ -2	-2 < RAI < 0	RAI = 0	0 < RAI < 2	2 ≤ RAI < 4	4 ≤ RAI

reflecting surface vegetation growth and is fundamental in ecosystem research (De Keersmaecker et al., 2017). In this study, EVI was derived from Landsat 5 (TM + MSS), Landsat 7 (TM + ETM), and Landsat 8 OLI products using equation (4) implemented in Google Earth Engine.

$$\mathrm{EVI} = \left[\frac{R_{\mathrm{NIR}} - R_{\mathrm{RED}}}{R_{\mathrm{NIR}} + C_1 R_{\mathrm{RED}} - C_2 R_{\mathrm{BLUE}} + 1}\right] 1 + L \quad (4)$$

Where;

EVI is the Enhanced Vegetation Index,

R_{NIR} is the reflection in the near-infrared region,

R_{RED} is the reflection in the red region,

R_{BLUE} is the blue band and

the values of L, C_1 and C_2 coefficients are -1, -6 and -7.5, respectively.

Relationship between climatic variables and vegetation

In this study, the impact of climate fluctuations on vegetation cover was assessed by examining the correlation of EVI with precipitation, temperature, SPI, and RAI. This investigation utilized the Pearson correlation coefficient. Additionally, a linear regression model was developed to explore the relationships between EVI and meteorological variables and indices (equation (5)).

$$Y = a + bX \quad (5)$$

where;

Y is the dependent variable (here is EVI),

a is the intercept,

b is the slope of the regression line, and

X is the independent variable (here is precipitation, temperature, SPI, and RAI).

The Mean Squared Error (MSE), Root Mean Square Error (RMSE), Mean Bias Error (MBE), and Mean Absolute Error (MAE) were employed to evaluate the performance of the regression models, in the validation phase to choose the optimal model.

Results

Precipitation and temperature

Fluctuations in precipitation showed a slightly decreasing trend, while the temperature changes reflect a slightly increasing trend (figure 3). From 1987 to 2022, each year experienced a reduction of 0.33 cm in precipitation and a rise of 0.05 °C increase in temperature.

From 1987 to 1988, the amount of precipitation had an increasing trend, then it decreased to 36.4 mm in 1989. From 1989 to 1993, the precipitation had an upward trend and reached 187.1 mm, the highest amount recorded in the study

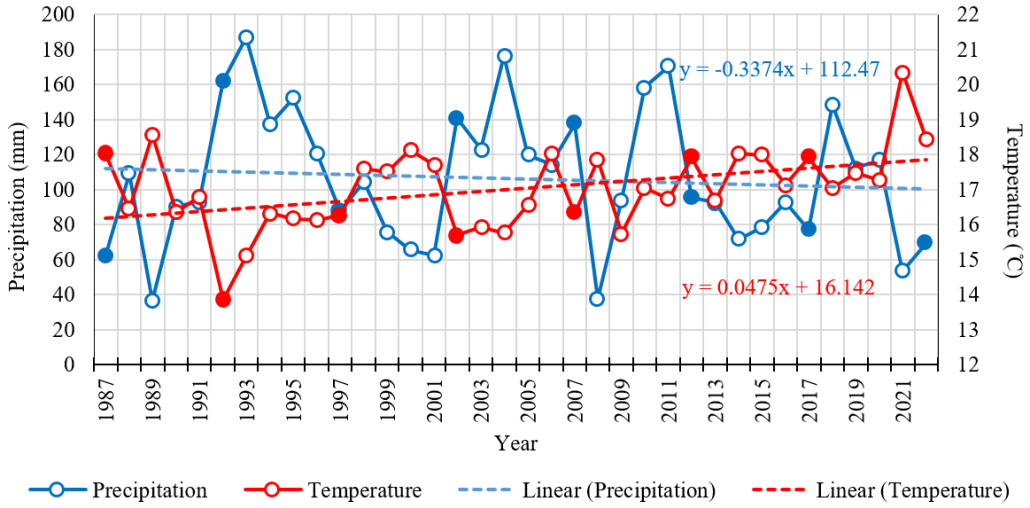

Figure 3. Trends of total precipitation (mm) and average temperature (°C) in Spring from 1987 to 2022.

period. Then, a decreasing trend begins, with precipitation reaching 62.4 mm by the year 2001. Then, it reached 176.1 mm in 2004. The trend from 2004 to 2008 (37.6 mm) is decreasing and after that, it is increasing up to 2011 (170.3 mm). From 2011 to 2022, the general trend of precipitation is decreasing, except for the period between 2018 and 2020. From 1987 to 1991, the temperature fluctuated and reached its lowest value in 1992 (13.8 °C). It then shows an increasing trend from 1992 to 2001. After a decrease in 2002 (15.7 °C), there is a general upward trend in temperature until 2022, with slight fluctuations.

Figure 4 indicates the maps of total precipitation in Spring in the study area. The southern parts of the West and East Azerbaijan provinces generally received more precipitation than the northern sides, except for the year 2022. The fluctuations in precipitation amount from 1987 to 2002 were observed while it decreased from 2002 to 2017. There was a significant increase in precipitation from 1987 to 1992 and 1997 to 2002 while it decreased from 1992 to 1997 and from 2002 onwards, the average annual precipitation in the study area showed a downward trend. The maximum amount of precipitation changed from 111.3 mm to 243.8 mm from 1987 to 2002. Additionally, the minimum values varied from 25.8 mm to 98.9 mm during this period. The maximum of 243.8 mm in 2002 reached 128.1 mm in 2017, and the minimum values changed from 98.9 mm to 29.9 mm during this period. The maximum amount of precipitation between 2017 and 2022 decreased from 128.1 mm to 119.0 mm, while the minimum amount of precipitation increased from 29.9 mm to 46.6 mm.

Figure 5 represents the maps of average temperature in Spring in the study area. It is observed that in 1987, the highest temperature was 21.4 °C and the lowest temperature was 15.3 °C. In 1992, the maximum temperature ranged from 17.5 °C to 10.6 °C, which showed a significant decrease compared to the previous five years. In 1997, an increase in temperature was observed so that the maximum temperature was 20.5 °C and the lowest was 13.0 °C. In 2002, the maximum temperature was 19.6 °C, while the minimum was 1.12 °C, and the maximum temperature was 19.7 °C and the minimum temperature was 13 °C in 2007. In 2012, an increase in temperature was observed so that the maximum range was 21.8 °C and the minimum was 14.2 °C. In 2017, the maximum and minimum temperatures were 20.7 and 14.7 °C, respectively. In 2022, an increase in temperature was observed so that the maximum temperature

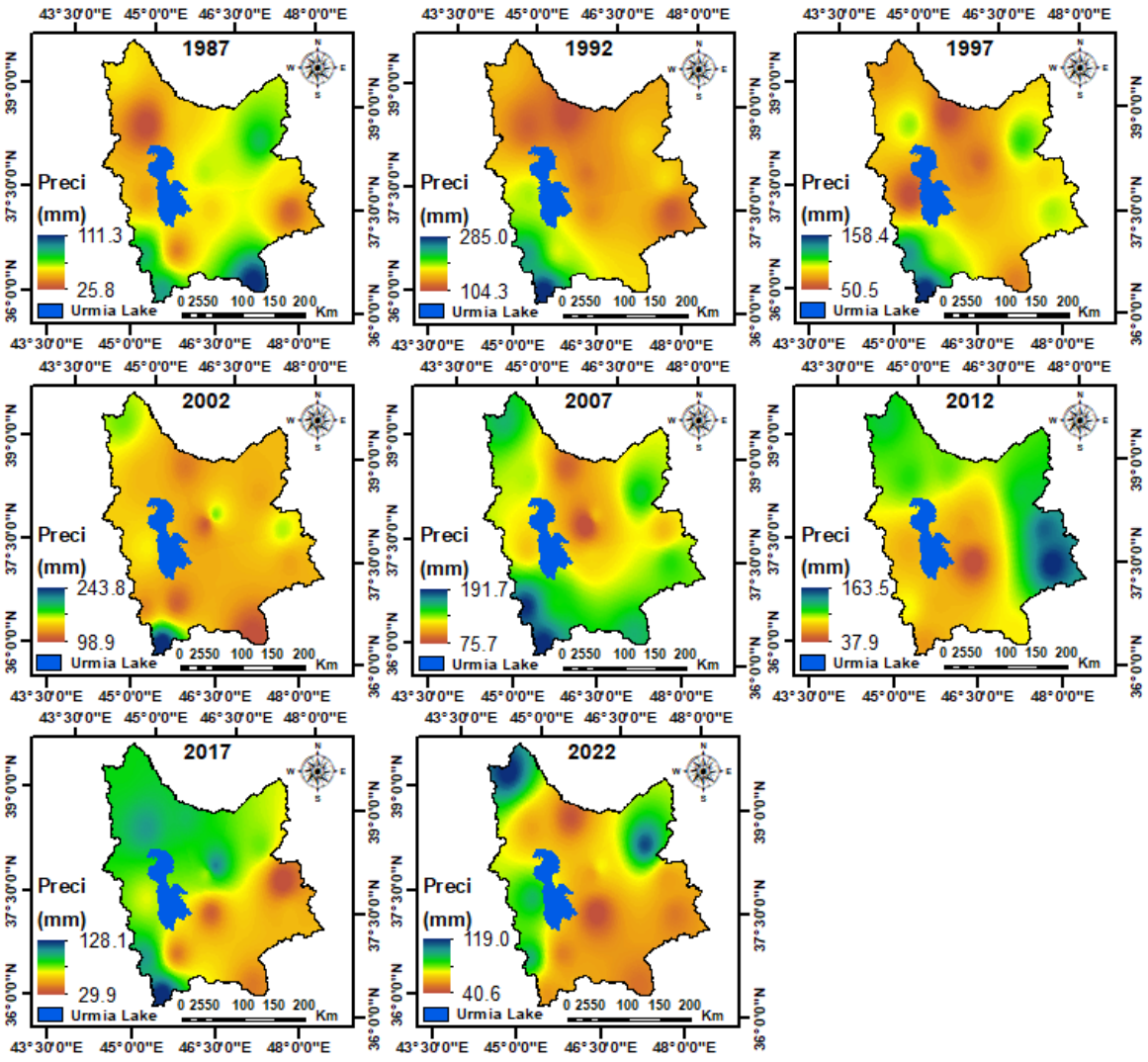

Figure 4. The maps of total precipitation in Spring in the West and East Azerbaijan provinces, Iran.

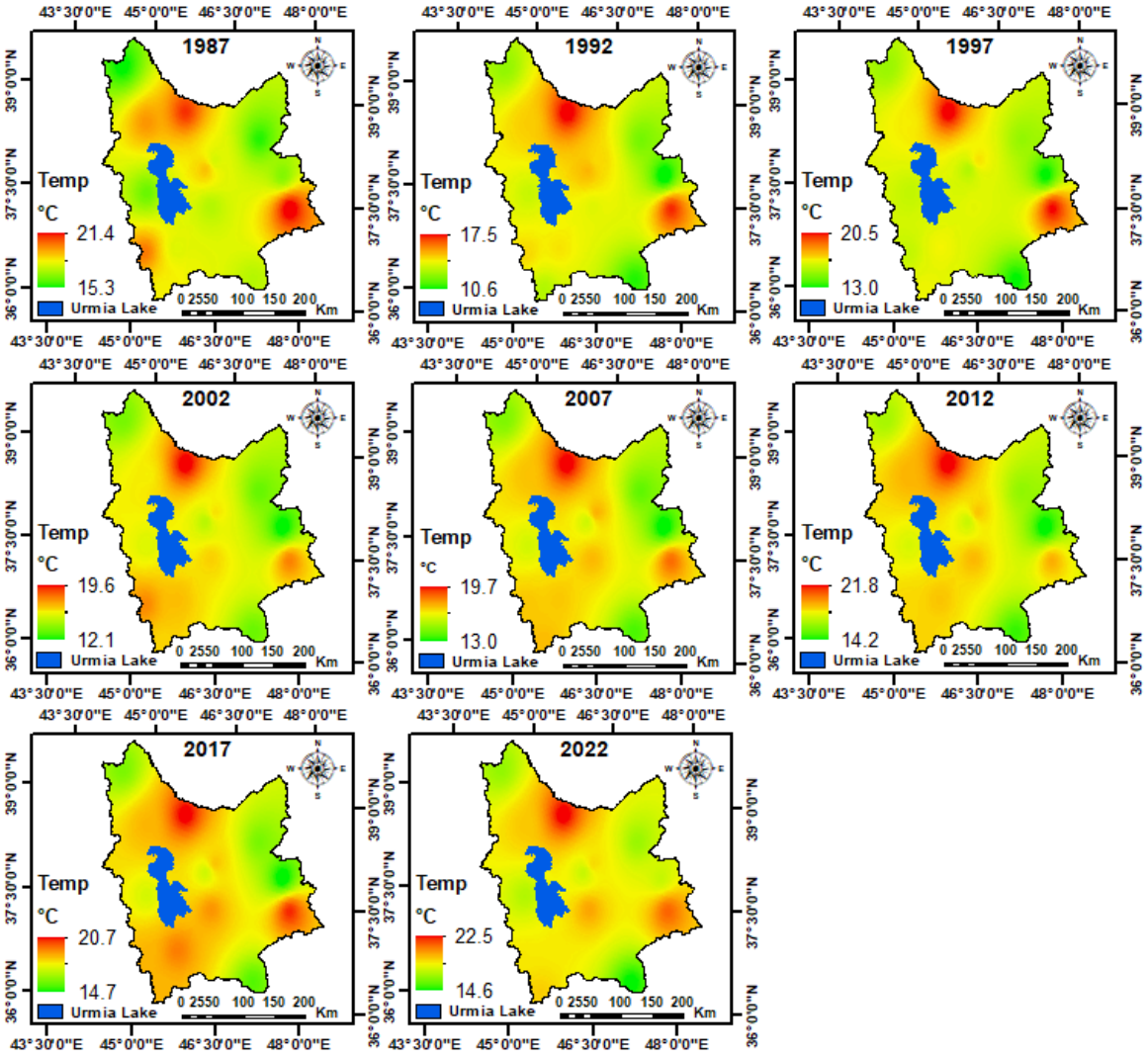

Figure 5. The maps of average temperature in Spring in the West and East Azerbaijan provinces, Iran.

was 22.5 °C and the lowest was 14.6 °C.

SPI and RAI

Figure 6 depicts drought and wet years based on SPI and RAI. The positive values indicate wet conditions and the negative values represent dry conditions. In general, both SPI and RAI had fluctuations with the same pattern and indicated a slightly decreasing trend from 1987 – 2022. From 1987 to 1992, the trend of these indices was increasing, with ranges of −1.48 (in 1989) to 1.11 (in 1992) and −3.48

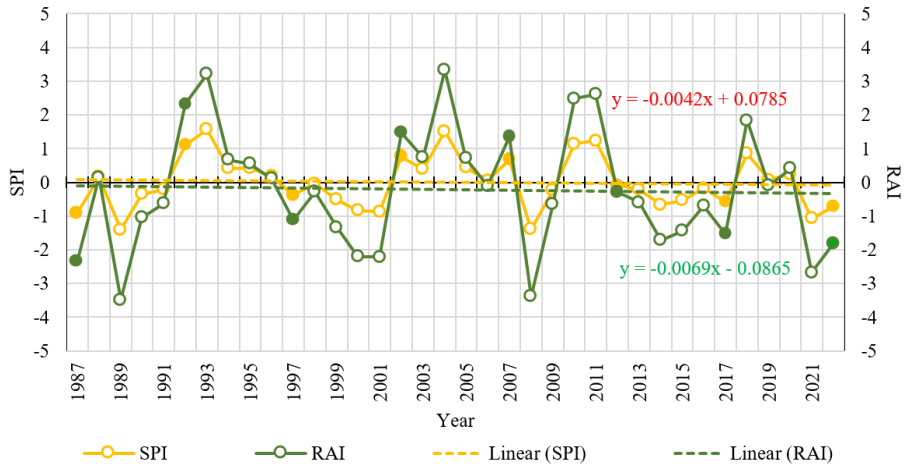

Figure 6. Trends of SPI and RAI in Spring from 1987 to 2022.

(in 1989) to 2.32 (in 1992) for SPI and RAI, respectively. During 1993 – 1997, the SPI and RAI ranged from −0.39 (in 1997) to 1.57 (in 1993) and −1.11 (in 1997) to 3.21 (in 1993), respectively, and the trends of these indices were steadily decreasing. From 1998 to 2002, the main trends were increasing although the values of SPI and RAI decreased from 1998 to 2001. The ranges of SPI and RAI varied from −0.87 (in 1989) to 0.76 (in 2002) and −2.22 (in 1989) to 1.48 (in 2002), respectively. From 2003 to 2007, the trends of SPI and RAI decreased and the range of −0.05 (in 2006) to 1.57 (in 2004) belongs to SPI and the range of −0.11 (in 2006) to 3.33 (in 2004) belongs to RAI. From 2012 to 2017, the SPI and RAI ranged from −1.40 (in 2008) to 1.23 (in 2011) and −3.39 (in 2008) to 2.61 (in 2011), respectively, and the main trends were decreasing although the values of SPI and RAI increased from 2008 to 2011. From 2013 to 2017, the trend of these indices was almost stable, with ranges of −0.66 (in 2014) to −0.21 (in 2013) and −1.72 (in 2014) to −0.59 (in 2013) for SPI and RAI, respectively. During 2018 – 2022, the SPI and RAI range from −1.07 (in 2021) to 0.85 (in 2018) and −2.68 (in 2021) to 1.83 (in 208), respectively, and the trends of these indices were steadily decreasing.

Figure 7 shows the maps of SPI in Spring in the West and East Azerbaijan provinces, Iran. In 1987, the highest SPI value was 0.24 and the lowest was −2.07. In 1992, the SPI ranged from 0.22 to 1.55, which shows a significant increase compared to the previous five-year period. In 1997, a decrease in SPI was observed so that it ranges from −1.40 to 0.33. In 2002, the maximum SPI was 1.83, while the minimum was 0.20. The maximum SPI in 2007 was 1.60 and the minimum was −0.18. In 2012, the SPI ranged from −0.07 to 2.10. In 2017, the maximum and minimum SPI were 0.40 and −1.43, respectively, and finally, in 2022, SPI values varied between −1.16 and 0.01.

Figure 8 indicates the maps of RAI in Spring in the West and East Azerbaijan provinces, Iran. In 1987, the highest RAI value was 0.63 and the lowest was −5.67. In 1997, an increase in SPI was found so that it varied between −4.05 to 0.92. In 2002, the RAI ranged from −0.52 to 4.54. In 2007, the maximum RAI was 4.49, while the minimum was −0.54. In 2012, the maximum SPI was 5.84, while the minimum was −2.81. In 2017, the RAI ranged from −3.58 to 0.98, and finally, the maximum SPI in 2022 was 0.03 and

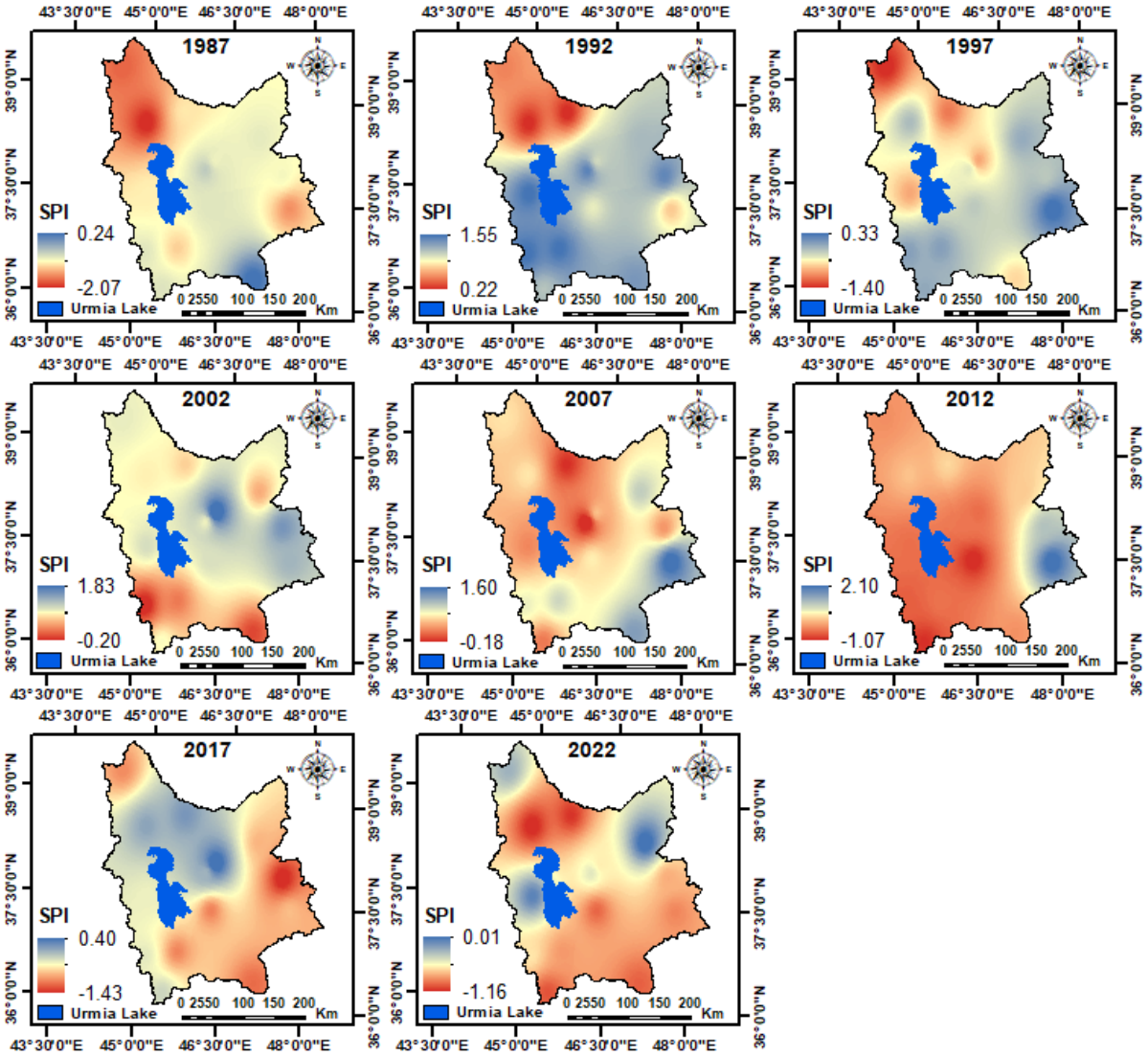

Figure 7. The SPI maps in Spring in the West and East Azerbaijan provinces.

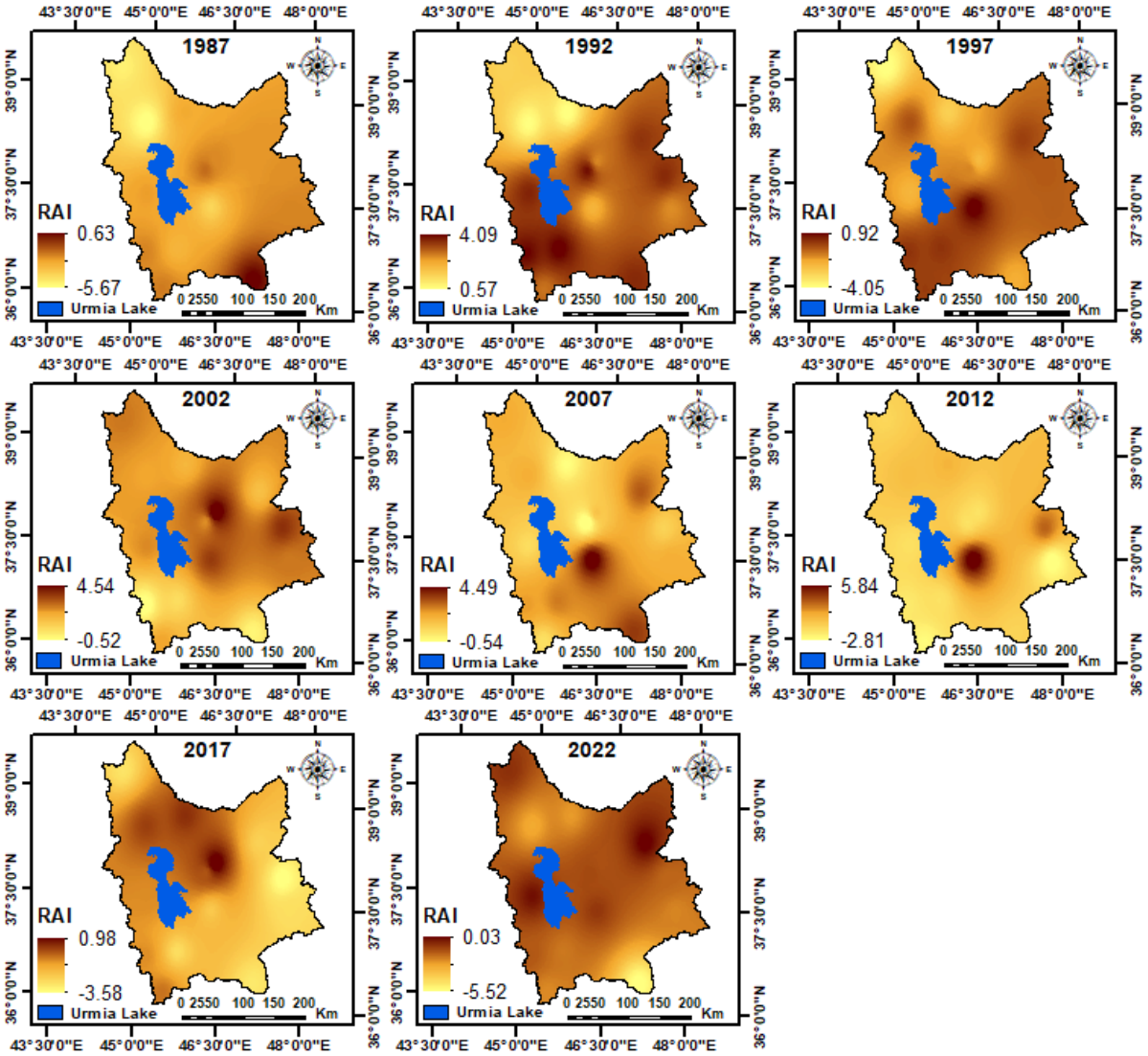

Figure 8. The RAI maps in Spring in the West and East Azerbaijan provinces.

the minimum was −5.52.

Figure 9 shows the spatial distribution of EVI across the West and East Azerbaijan provinces, Iran in five-year intervals from 1987 to 2022. Among the LULC classes, the urban area, rock, salt land, and water body were identified as non-vegetation types and excluded from the maps. As shown in 1987, the maximum EVI was 0.80, while the lowest value was −0.27. In 1992, the maximum EVI was 1.01 and its minimum was −0.46. In 1997, EVI decreased compared to the previous period so that its maximum value is 0.82 and its minimum value was −1.11. In 2002, there was not much progress in terms of EVI and the maximum value of EVI equals to 0.99 and the minimum value was −0.98. In 2007, the maximum and minimum of EVI were 1.36 and −1.47, respectively, while the maximum and minimum were reported as 0.93 and −1.56 respectively, in 2012. In 2017, the EVI ranged between −1.70 and 1.12, and in 2022, the EVI varied from −0.53 to 2.03.

Table 6 represents the mean value along with the standard deviation of EVI maps for different LULC types. The urban area, rock, salt land, and water bodies were considered no-vegetation types and excluded from the mas. The results showed that EVI values were typically higher in forest classes compared to rangeland classes and agricultural land. In addition, poor rangeland had generally the lowest EVI values across the study period.

The EVI values in agricultural land exhibit relatively minor fluctuations, ranging from 0.17 in 2022 to 0.27 in 2017. In dense forests, the highest was recorded in 1992 (0.48), while the lowest EVI value occurred in 2022 (0.26). In moderate forests, EVI mean values range from 0.20 (in 2022) to 0.33 (in 2017). The highest mean value of EVI in sparse forest was 0.31 (in 2017), while the lowest is 0.20 (in 2022). In good rangeland, the highest EVI value was found in 2017 (0.25), and the lowest occurred in 2022 (0.15). The highest and lowest mean values of EVI in moderate rangeland were found 0.22 (in 2017) and 0.15 (in 1997 and 2022), respectively. EVI values in poor rangeland varied between 0.10 (in 1997) and 0.18 (in 2017).

The standard deviation of EVI indicates that the highest variations around the mean values predominantly occurred in dense forests, which had typically high standard deviation values. While the lowest variations were generally observed in the poor rangelands, with low standard deviation values.

Table 6. Mean value and standard deviation of EVI for different LULC types.

LULC class	1987	1992	1997	2002	2007	2012	2017	2022
Agricultural land	0.20±0.09	0.21±0.11	0.21±0.10	0.24±0.13	0.22±0.09	0.23±0.10	0.27±0.12	0.17±0.08
Dense forest	0.36±0.12	0.49±0.15	0.38±0.10	0.30±0.13	0.34±0.08	0.44±0.10	0.48±0.11	0.26±0.08
Moderate forest	0.25±0.09	0.29±0.12	0.25±0.09	0.24±0.11	0.25±0.08	0.31±0.09	0.33±0.10	0.20±0.05
Spare forest	0.24±0.07	0.25±0.09	0.24±0.08	0.29±0.12	0.24±0.07	0.28±0.07	0.31±0.07	0.20±0.05
Good rangeland	0.18±0.06	0.22±0.08	0.16±0.07	0.20±0.16	0.23±0.10	0.23±0.08	0.25±0.07	0.15±0.03
Moderate rangeland	0.17±0.06	0.16±0.07	0.15±0.06	0.17±0.11	0.17±0.07	0.19±0.07	0.22±0.07	0.15±0.03
Poor rangeland	0.12±0.04	0.12±0.05	0.10±0.04	0.14±0.10	0.13±0.06	0.13±0.06	0.18±0.06	0.14±0.03
Total area	0.17±0.08	0.19±0.10	0.17±0.09	0.20±0.13	0.19±0.09	0.21±0.10	0.18±0.10	0.16±0.04

Relationship between EVI with precipitation, temperature, SPI, and RAI

Figure 10 illustrates the correlation between EVI and various climatic variables and indices. The correlation coefficients indicate a positive relationship between EVI and precipitation ($r = 0.53$), as well as with both SPI ($r = 0.57$) and RAI ($r = 0.61$), are positive. While the correlation between EVI and temperature was low and non-significant

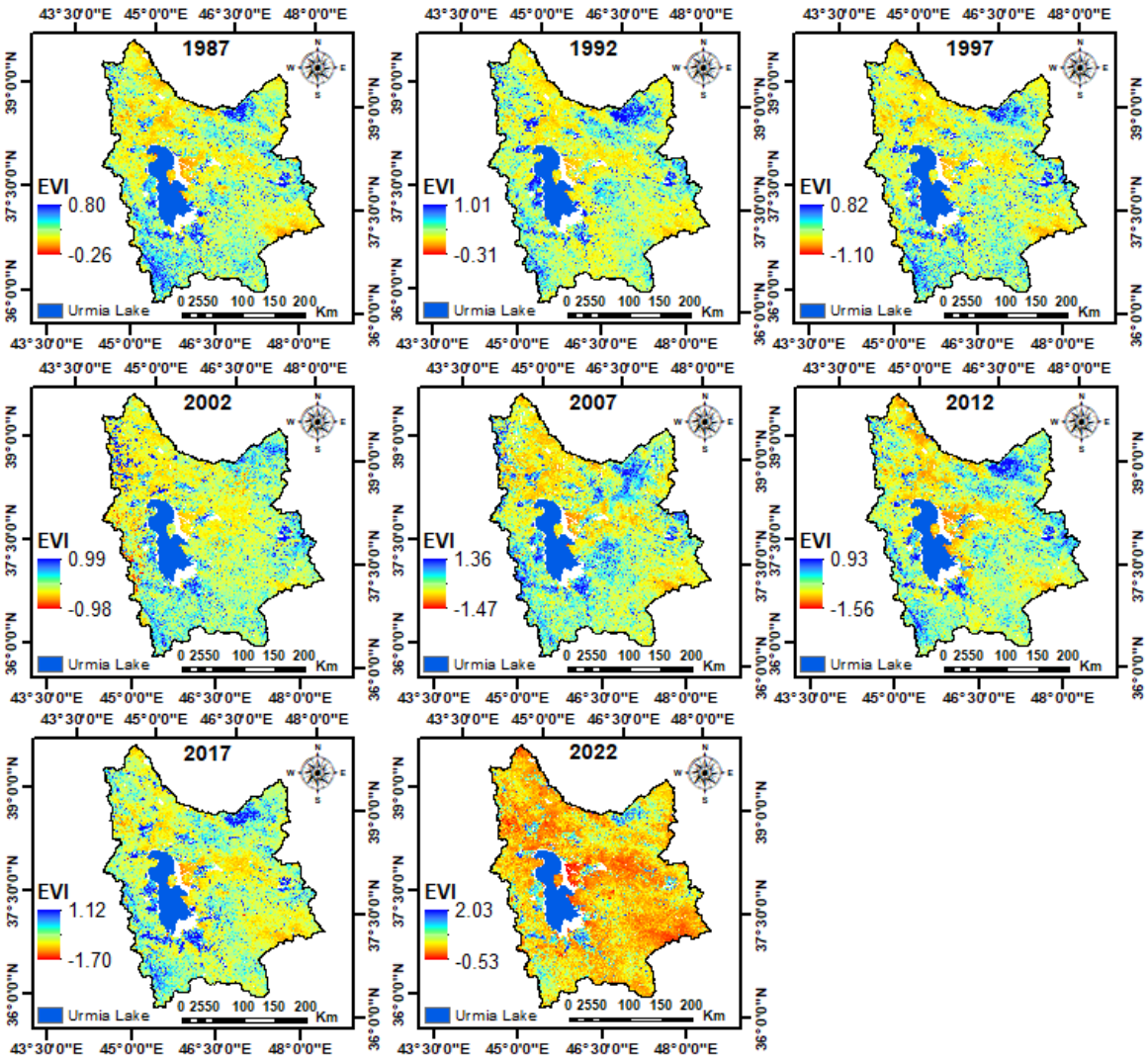

Figure 9. The maps of average EVI in Spring in the West and East Azerbaijan provinces.

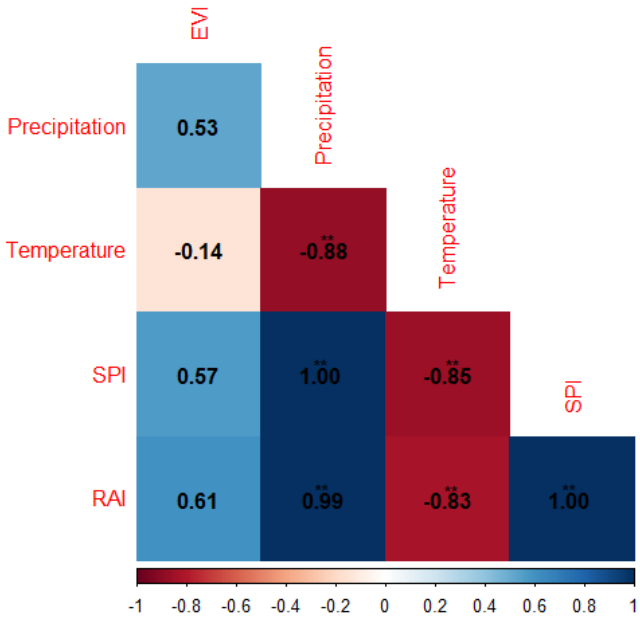

Figure 10. Correlation matrix among EVI, precipitation, temperature, SPI, and RAI.

($r = -0.14$). The correlation values between precipitation and temperature ($r = -0.88$), SPI and temperature ($r = -0.85$), and RAI and temperature ($R = -0.83$) were negative. Additionally, a strong positive correlation coefficient was noted between precipitation and meteorological indices (SPI ($r = 1.00$) and RAI ($r = 0.99$)), with consistently high correlation values.

Table 7 presents the regression models that describe the relationship between EVI and meteorological variables and indices, and highlights the most accurate models for different LULC types. The slopes of the regression models for the relationship between EVI and precipitation, SPI, and RAI were positive across all LULC types, except for moderate and poor rangelands. In contrast, the slope of the regression models for EVI and temperature was negative in all LULC types, except for moderate rangeland and poor rangeland. According to the statistics, the estimation of EVI in all LULC types was suitable based on the SPI (with the lowest values of MSE and RMSE). Meanwhile, in moderate and poor rangelands, RAI also provides an appropriate model, in addition to SPI.

The RMSE values for the most accurate model in agricultural land, dense forest, moderate forest, spare forest, good rangeland, moderate rangeland, and poor rangeland were 0.0174, 0.0767, 0.0402, 0.0317, 0.0314, 0.0204, and 0.0209, respectively.

Discussion

Understanding how vegetation responds to environmental factors such as precipitation and temperature is essential for assessing ecosystem dynamics and structure. Drought conditions can restrict and endanger vegetation cover and affect the water resources that vegetation relies on. Therefore, the availability of adequate water, which is crucial for vegetation growth, is a key factor. This study examined vegetation dynamics and their relationship to fluctuations in climatic variables and indices in the West and East Azerbaijan provinces, Iran.

Precipitation and temperature are primary factors directly influencing the trend of wet or dry conditions (Eskandari Damaneh et al., 2024), it is essential and urgent to investigate changes in precipitation patterns due to climate fluctuations, which affect water availability for vegetation. The results indicated a decreasing trend for precipitation and an increasing trend in temperature, which aligns with the findings of Dehghani Sargazi et al. (2021). Some researchers have reported a decrease in precipitation due to a reduction in the number of rainy days (Batisani and Yarnal, 2010).

The results of meteorological variables indicated that changes in vegetation cover performance are interpretable due to fluctuations in climatic variations. Generally, the changes in precipitation indicated a slightly decreasing trend, while the fluctuations in temperature trend showed a slightly increasing trend. Vegetation index (EVI) showed a positive correlation with precipitation ($r = 0.53$), while its correlation with temperature was not significant. It confirms that vegetation cover improves with increasing wetter years while decreasing vegetation cover occurs in drier years. In other words, fluctuations in climatic variables directly cause changes in vegetation performance.

SPI and RAI have been introduced as rain-based indicators (Sa'adi et al., 2022), enabling them to play an effective role not only in understanding regional climate and precipitation but also in strategic planning and decision-making in various sectors of society, such as agriculture, water resources, and urban planning (Silva et al., 2022). The results obtained regarding the meteorological indicators clearly showed that the dry and wet conditions in the RAI were more intense than the SPI. Furthermore, the effectiveness of these two indices in determining the change process of the drought and drought periods of the current study was confirmed (Montaseri et al., 2016).

In general, increasing drought conditions in recent years may be attributed to human activities, deforestation, and

land-use changes leading to the emission of large amounts of greenhouse gases and consequently, an increase in predicted temperatures, which could potentially result in more intense and frequent heatwaves and exacerbate drought periods (Sheffield and Wood, 2008). This is while the increase in the frequency or magnitude of severe hydrological events, heatwaves, and cold waves may negatively impact ecosystem health and consequently disrupt the stability of natural resources (Ledger and Milner, 2015).

The findings also showed that the slopes of the linear regression models, which show the relationship between EVI and precipitation, SPI, and RAI, were positive in all LULC types, except for moderate and poor rangelands. Conversely, the slope of regression models for EVI and temperature were negative across all LULC types, with the exceptions of moderate rangeland and poor rangeland. This could be due to the presence of these rangelands at higher elevations, where the generally low temperatures limit vegetation growth and development.

Additionally, based on the results for the validation of linear regression models, SPI proved to be more effective in the estimation and prediction of vegetation density in the study area. However, RAI showed almost the same results as SPI in moderate and poor rangelands.

Table 7. Regression models of EVI as dependent variable with meteorological variables precipitation (P), temperature (T), SPI, and RAI as independent variables.

LULC type	Relationship	Regression model	MSE	RMSE	MBE	MAB
Agricultural land	EVI vs P	EVI = (0.0001×P) + 0.2065	0.0009	0.0305	-0.0111	0.0228
	EVI vs T	EVI = (-0.0011×T) + 0.2355	0.0011	0.0335	0.0177	0.02667
	EVI vs SPI	**EVI = (0.0058×SPI) + 0.2177**	**0.0003**	**0.0174**	**0.0014**	**0.0222**
	EVI vs RAI	EVI = (0.0021×RAI) + 0.2176	0.0008	0.0283	0.0005	0.0222
Dense forest	EVI vs P	EVI = (0.0004×P) + 0.3391	0.0077	0.0877	-0.0406	0.0715
	EVI vs T	EVI = (-0.0148×T) + 0.6257	0.0639	0.2528	0.2402	0.2402
	EVI vs SPI	**EVI = (0.0158×SPI) + 0.3798**	**0.0059**	**0.0767**	**0.0060**	**0.0669**
	EVI vs RAI	EVI = (0.0052×RAI) + 0.3796	0.0060	0.0773	0.0017	0.0665
Moderate forest	EVI vs P	EVI = (0.0001×P) + 0.2495	0.0019	0.0432	-0.0152	0.0319
	EVI vs T	EVI = (-0.0034×T) + 0.3209	0.0047	0.0685	0.0552	0.0567
	EVI vs SPI	**EVI = (0.0065×SPI) + 0.2647**	**0.0016**	**0.0402**	**0.0017**	**0.0350**
	EVI vs RAI	EVI = (0.002×RAI) + 0.2646	0.0016	0.0404	0.0004	0.0349
Spare forest	EVI vs P	EVI = (0.0001×P) + 0.2396	0.0013	0.0357	-0.0160	0.0259
	EVI vs T	EVI = (-0.0009×T) + 0.2707	0.0012	0.0352	0.0148	0.0305
	EVI vs SPI	**EVI = (0.0092×SPI) + 0.2562**	**0.0010**	**0.0317**	**0.0029**	**0.0272**
	EVI vs RAI	EVI = (0.0031×RAI) + 0.256	0.0010	0.0318	0.0011	0.0269
Good rangeland	EVI vs P	EVI = (0.0003×P) + 0.166	0.0023	0.0478	-0.0358	0.0398
	EVI vs T	EVI = (-0.0038×T) + 0.264	0.0048	0.0691	0.0614	0.0614
	EVI vs SPI	**EVI = (0.0167×SPI) + 0.2028**	**0.0010**	**0.0314**	**0.0043**	**0.0278**
	EVI vs RAI	EVI = (0.0064×RAI) + 0.2026	0.0010	0.0316	0.0020	0.0281
Moderate rangeland	EVI vs P	EVI = (-0.00004×P) + 0.1741	0.0004	0.0207	0.0037	0.0174
	EVI vs T	EVI = (0.0034×T) + 0.1128	0.0037	0.0605	-0.0570	0.0570
	EVI vs SPI	**EVI = (-0.0011×SPI) + 0.1704**	**0.0004**	**0.0204**	**-0.0002**	**0.0154**
	EVI vs RAI	**EVI = (-0.0006×RAI) + 0.1703**	**0.0004**	**0.0204**	**-0.0002**	**0.0154**
Poor rangeland	EVI vs P	EVI = (-0.00002×P) + 0.1334	0.0004	0.0210	0.0017	0.0156
	EVI vs T	EVI = (0.0049×T) + 0.0473	0.0074	0.0863	-0.0837	0.0837
	EVI vs SPI	**EVI = (-0.0001×SPI) + 0.1316**	**0.0004**	**0.0209**	**-0.0001**	**0.0152**
	EVI vs RAI	**EVI = (-0.00003×RAI) + 0.1317**	**0.0004**	**0.0209**	**0.0001**	**0.0152**

The bold regression equations are the most accurate regression for different LULC types according to lower values of MSE, RMSE, MBE, and MAB.

Conclusion

The spatial distribution of EVI across the West and East Azerbaijan provinces showed variations during 1987 – 2022, attributed partly to temperature and precipitation changes. The findings of current research suggested that spatial changes in temperature and precipitation can lead to changes in habitat equilibrium and behavior of animal and plant species. West and East Azerbaijan provinces are not exempt from this phenomenon due to their topographical status and their rich environmental and plant diversity, which are currently compatible with climate. Therefore, long-term fluctuations and variability in regional climate factors can have significant environmental and agricultural consequences for these regions. Based on the results, the vegetation showed a positive correlation with precipitation; on the other hand, it has a slight negative correlation with temperature. Moreover, the SPI exhibited more suitable results in estimating vegetation conditions in the West and East Azerbaijan provinces.

In conclusion, it is inferred that for drought monitoring, SPI and RAI can be used in conjunction with other environmental indices and approaches such as vulnerability assessment and remote sensing techniques. Moreover, focusing on the meteorological variables trends during strategic decision-making and planning should not be overlooked. While the findings were convincing, there are some unavoidable limitations. Specifically, this study did not examine how human activities, such as changes in land use/cover affect vegetation dynamics. Therefore, it is suggested that future research should explore the role of the human in both degrading and restoring vegetation cover, given their significant impact on plant growth. Additionally, future studies could focus on predicting future climate conditions and land use patterns in the studied region and assessing the socio-economic vulnerability linked to these changes over time.

Authors Contributions
All authors have contributed equally to prepare the paper.

Availability of Data and Materials
The data that support the findings of this study are available from the corresponding author upon reasonable request.

Conflict of Interests
The authors declare that they have no known competing financial interests or personal relationships that could have appeared to influence the work reported in this paper.

References

Ahmadi S., Azarnivand H., Khosravi H., Dehghan P., Behrang Manesh M. (2019) Assessment of the effect of drought and land use change on vegetation using Landsat data. *Desert* 24 (1): 23–31. DOI: https://doi.org/10.22059/JDESERT.2019.72432.

Amiri M. A., Gocic M. (2023) Analysis of temporal and spatial variations of drought over Serbia by investigating the applicability of precipitation-based drought indices. *Theoretical and Applied Climatology* 154 (1): 261–274. DOI: https://doi.org/10.1007/s00704-023-04554-6.

Aryal A., Maharjan M., Talchabhadel R., Thapa B. R. (2022) Characterizing meteorological droughts in Nepal: A comparative analysis of standardized precipitation index and rainfall anomaly index. *Earth* 3 (1): 409–432. DOI: https://doi.org/10.3390/earth3010025.

Bagheri S., Tamartash R., Jafari M., Tatian M. R., Malekian A. (2022) The effects of drought on vegetation using satellite remote sensing and meteorological data (case study: Qazvin plain). *Journal of Range and Watershed Management* 75 (1): 1–18. DOI: https://doi.org/10.22059/jrwm.2020.277200.1361.

Batisani N., Yarnal B. (2010) Rainfall variability and trends in semi-arid Botswana: Implications for climate change adaptation policy. *Applied Geography* 30 (4): 483–489. DOI: https://doi.org/10.1016/j.apgeog.2009.10.007.

Buras A., Rammig A., Zang C. S. (2020) Quantifying impacts of the 2018 drought on European ecosystems in comparison to 2003. *Biogeosciences* 17 (6): 1655–1672. DOI: https://doi.org/10.5194/bg-17-1655-2020.

Darvand S., Eskandari Damaneh H., Eskandari Damaneh H., Khosravi H. (2021) Prediction of the changing trend of temperature and rainfall in the future period and its impact on desertification. *Water and Soil Management and Modelling* 1 (1): 53–66. DOI: https://doi.org/10.22098/mmws.2021.1181.

Dastigerdi M., Nadi M., Sarjaz M. R., Kiapasha K. (2024) Trend analysis of MODIS NDVI time series and its relationship to temperature and precipitation in Northeastern Iran. *Environmental Monitoring and Assessment* 196 (4): 1–16. DOI: https://doi.org/10.1007/s10661-024-12463-y.

De Keersmaecker W., Lhermitte S., Hill M. J., Tits L., Coppin P., Somers B. (2017) Assessment of regional vegetation response to climate anomalies: A case study for Australia using GIMMS NDVI time series between 1982 and 2006. *Remote Sensing* 9 (1): 34. DOI: https://doi.org/10.3390/rs9010034.

Dehghan Rahimabadi P., Abdolshahnejad M., Heydari Alamdarloo E., Azarnivand H. (2024) Vegetation dynamics assessment: Remote sensing and statistical approaches to determine the contributions of driving factors. *Journal of the Indian Society of Remote Sensing* 52:1969–1984. DOI: https://doi.org/10.1007/s12524-024-01917-y.

Dehghan Rahimabadi P., Azarnivand H. (2023) Assessment of the effect of climate fluctuations and human activities on vegetation dynamics and its vulnerability. *Theoretical and Applied Climatology* 153 (1): 771–786. DOI: https://doi.org/10.1007/s00704-023-04504-2.

Dehghan Rahimabadi P., Azarnivand H., Khosravi H., Zehtabian G., Moghaddam Nia A. (2018) Design of agricultural ecological and rangeland capability model using an integrated approach of FUZZY-AHP (A case study: Eshtehard city). *Journal of Range and Watershed Management* 71 (1): 11–24. DOI: https://doi.org/10.22059/jrwm.2017.238015.1147.

Dehghan Rahimabadi P., Azarnivand H., Khosravi H., Zehtabian G., Moghaddamnia A. (2021) An ecological agricultural model using fuzzy AHP and PROMETHEE II approach. *Desert* 26 (1): 71–83. DOI: https://doi.org/10.22059/jdesert.2020.303314.1006778.

Dehghani Sargazi H., Bazrafshan O., Zamni H. (2021) Investigation of the effect of meteorological-agricultural drought on rainfed wheat yield in Iran using SPEI. *Nivar* 45 (114-115): 15–26. https://nivar.irimo.ir/article_136292.html

Eskandari Damaneh H., Eskandari Damaneh H., Sayadi Z., Khoorani A. (2021) Evaluation of spatiotemporal changes and correlations of aerosol optical depth, NDVI and climatic data over Iran. *Iranian Journal of Range and Desert Research* 28 (4): 772–786. DOI: https://doi.org/10.22092/ijrdr.2021.125252.

Eskandari Damaneh H., Khosravi H., Eskandari Damaneh H. (2024) Investigating the land use changes effects on the surface temperature using Landsat satellite data. *Remote Sensing of Soil and Land Surface Processes,* 155–174. DOI: https://doi.org/10.1016/B978-0-443-15341-9.00007-1.

Eskandari Damaneh H., Zehtabian G., Khosravi H., Azarnivand H., Barati A. (2022) Investigating the influence of drought on the trend of vegetation changes in arid and semiarid regions, using remote sensing technique: A case study of Hormozgan Province. *Desert Ecosystem Engineering* 9 (28): 13–28. DOI: https://doi.org/10.22052/DEEJ.2020.9.28.11.

Farajnia A., Moravej K. (2020) Agro-climatic zoning of saffron culture in East Azarbayjan province. *Journal of Saffron Research* 7 (2): 252–267. DOI: https://doi.org/10.22077/jsr.2018.1445.1057.

Hasan H. H., Razali S. F. M., Muhammad N. S., Hamzah F. M. (2021) Assessment of probability distributions and analysis of the minimum storage draft rate in the equatorial region. *Natural Hazards and Earth System Sciences* 21:1–19. DOI: https://doi.org/10.5194/nhess-21-1-2021.

Heydari Alamdarloo E., Khosravi H., Dehghan Rahimabadi P., Ghodsi M. (2021) The effect of climate fluctuations on vegetation dynamics in west and northwest of Iran. *Desert Ecosystem Engineering Journal* 3 (2): 19–28. https://jdee.kashanu.ac.ir/article_111533.html

Heydari Alamdarloo E., Khosravi H., Nasabpour S., Gholami A. (2020) Assessment of drought hazard, vulnerability and risk in Iran using GIS techniques. *Journal of Arid Land* 12:984–1000. DOI: https://doi.org/10.1007/s40333-020-0096-4.

Hui-Mean F., Yusop Z., Yusof F. (2018) Drought analysis and water resource availability using standardized precipitation evapotranspiration index. *Atmospheric Research* 201:102–115. DOI: https://doi.org/10.1016/j.atmosres.2017.10.014.

Kartal S., Iban M. C., Sekertekin A. (2024) Next-level vegetation health index forecasting: A ConvLSTM study using MODIS Time Series. *Environmental Science and Pollution Research* 31 (12): 18932–18948. DOI: https://doi.org/10.1007/s11356-024-32430-x.

Khan A. A., Zhao Y., Khan J., Rahman G., Rafiq M., Moazzam M. F. U. (2021) Spatial and temporal analysis of rainfall and drought conditions in Southwest Xinjiang in Northwest China, using various climate indices. *Earth Systems and Environment* 5 (2): 201–216. DOI: https://doi.org/10.1007/s41748-021-00226-5.

Ledger M. E., Milner A. M. (2015) Extreme events in running waters. *Freshwater Biology* 60 (12): 2455–2460. DOI: https://doi.org/10.1111/fwb.12673.

Medeiros G. C. S. D., Silva S. M. O. D. (2024) Propagation from Meteorological Drought to Hydrological Drought Using SPI and SPEI Combined with the Adapted Threshold Level Method. *EGUsphere* 2024:1–32. DOI: https://doi.org/10.5194/egusphere-2024-813.

Montaseri M., Amirataee B., Khalili K. (2016) Identification of trends in spatial and temporal dry and wet periods in northwest Iran based on SPI and RAI indices. *Journal of Water and Soil* 30 (2): 655–671. DOI: https://doi.org/10.22067/JSW.V30I2.39679.

Sa'adi Z., Yusop Z., Alias N. E. (2022) Inter-comparison on the suitability of rain-based meteorological drought in Johor River Basin, Malaysia. *KSCE Journal of Civil Engineering* 26 (5): 2519–2537. DOI: https://doi.org/10.1007/s12205-022-1481-7.

Saberi A., Soltani-Gerdefaramarzi S. (2017) Evaluation of geostatistical methods in mapping the severity of the drought in West Azerbaijan province, Iran. *Irrigation and Water Engineering* 7 (3): 151–165. https://www.waterjournal.ir/article_74074.html?lang=en

Sheffield J., Wood E. F. (2008) Projected changes in drought occurrence under future global warming from multi-model, multi-scenario, IPCC AR4 simulations. *Climate dynamics* 31:79–105. DOI: https://doi.org/10.1007/s00382-007-0340-z.

Silva T. R. B. F., Santos C. A. C. D., Silva D. J. F., Santos C. A. G., Silva R. M. da, Brito J. I. B. de (2022) Climate indices-based analysis of rainfall spatiotemporal variability in Pernambuco State, Brazil. *Water* 14 (14): 2190. DOI: https://doi.org/10.3390/w14142190.

Tirivarombo S. O. D. E., Osupile D., Eliasson P. (2018) Drought monitoring and analysis: Standardized precipitation evapotranspiration index (SPEI) and standardized precipitation index (SPI). *Physics and Chemistry of the Earth, Parts A/B/C* 106:1–10. DOI: https://doi.org/10.1016/j.pce.2018.07.001.

Vicente-Serrano S. M., Beguería S., López-Moreno J. I. (2010) A multiscalar drought index sensitive to global warming: The standardized precipitation evapotranspiration index. *Journal of Climate* 23 (7): 1696–1718. DOI: https://doi.org/10.1175/2009JCLI2909.1.

Wu K., Chen J., Yang H., Yang Y., Hu Z. (2023) Spatiotemporal variations in the sensitivity of vegetation growth to typical climate factors on the Qinghai–Tibet Plateau. *Remote Sensing* 15 (9): 2355. DOI: https://doi.org/10.3390/rs15092355.

Yeh H. F. (2019) Using integrated meteorological and hydrological indices to assess drought characteristics in southern Taiwan. *Hydrology Research* 50 (3): 901–914. DOI: https://doi.org/10.2166/nh.2019.120.

Zhan Y., Fan J., Meng T., Li Z., Yan Y., Huang J., Chen D., Sui L. (2021) Analysis of vegetation cover changes and the driving factors in the mid-lower reaches of Hanjiang River Basin between 2001 and 2015. *Open Geosciences* 13 (1): 675–689. DOI: https://doi.org/10.1515/geo-2020-0256.

Zhang Q., Gu L., Liu Y., Zhang Y. (2024) Spatio-temporal dynamics of normalized difference vegetation index and its response to climate change in Xinjiang, 2000–2022. *Forests* 15 (2): 370. DOI: https://doi.org/10.3390/f15020370.

Zhang Y. X., Wang Y. K., Fu B., Dixit A. M., Chaudhary S., Wang S. (2020) Impact of climatic factors on vegetation dynamics in the upper Yangtze River basin in China. *Journal of Mountain Science* 17 (5): 1235–1250. DOI: https://doi.org/10.1007/s11629-019-5550-4.

Zhou Y., Zhou P., Jin J., Wu C., Cui Y., Zhang Y., Tong F. (2022) Drought identification based on Palmer drought severity index and return period analysis of drought characteristics in Huaibei Plain China. *Environmental Research* 212:113163. DOI: https://doi.org/10.1016/j.envres.2022.113163.